Research Article

Yibo Gao, Jianlin Luo*, Jigang Zhang, Xiaoyang Zhou, Fei Teng, Changquan Liu, and Xijie Sun

Repairing performances of novel cement mortar modified with graphene oxide and polyacrylate polymer

https://doi.org/10.1515/ntrev-2022-0091
received November 21, 2021; accepted February 17, 2022

Abstract: Most cementitious repair materials have non-ignorable drawbacks such as low strength, insufficient bonding, and low anti-permeability. Although the bonding and anti-permeability of repair mortars modified by polymer will be substantially improved, the compressive strength and component integrity will be decreased. Hereby six groups of cement mortars modified by varied dosages of Graphene Oxide (GO) and PA copolymer (GOPARMs) were prepared. The flexural strength (f_t), compressive strength (f_c), f_t/f_c, bond strength (f_b), and chloride ion migration coefficient (λ_c) of GOPARMs were systematically studied by axial compressive, three-bending, pull-out, RCM method, along with microstructure analysis. When GO and PA dosages are fixed at 0.03 and 5 wt%, respectively, the f_t, f_c, f_t/f_c, f_b, and λ_c of GOPARMs reach the best comprehensive performances, which are 6.4, 46.5, 0.14, 6.73 MPa, and 1.179×10^{-12} m^2/s. Compared with the control mortar, the f_t, f_c, f_t/f_c, and f_b of GOPARMs are improved by 5.7, 12.3, 7, and 103%, respectively, and the corresponding λ_c is dramatically reduced by 40.4%. Scanning electron microscope (SEM) shows that trace of GO can play a template nucleation effect on the hydration products' morphology and microstructure of GOPARMs. Meanwhile, cured PA polymer can form hydrophobic film and fill the interfacial pores among hydration products, finally superior repairing performances of GOPARMs with optimal mix can be achieved.

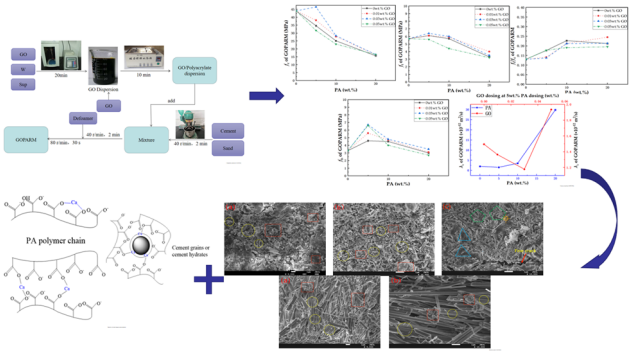

Graphical abstract

Keywords: structural repair, interface bonding, nano-modified polymer mortar

1 Introduction

With the large-scale construction of concrete infrastructure in China, cement production has increased year by year, where large amounts of carbon dioxide greenhouse gas are emitted. The concrete structure under harsh environment cannot reach the expected durability, which will shorten its service life. However, rebuilding and reconstruction will bring forth more carbon emissions. Actually, using high-performance repair materials to repair and strengthen the original damaged parts or cracks of concrete structure is more cost-effective and eco-environmental compared to the traditional rebuilding and reconstruction. The repaired structure can continuously hinder the invasion of external harmful substances and the service life can be effectively prolonged [1–9].

In order to achieve good compatibility with the original concrete structure, the cement-based repair mortars are often chosen as the repair materials [10–15]. But lots

* **Corresponding author: Jianlin Luo,** School of Civil Engineering, Qingdao University of Technology, Qingdao 266520, China; Collaborative Innovation Center of Engineering Construction and Safety in Shandong Blue Economic Zone, Qingdao 266033, China, e-mail: lawjanelim2009hit@gmail.com, lawjanelim@qut.edu.cn, tel: +86 532 8507 1605, fax: +86 532 8507 1605
Yibo Gao, Xiaoyang Zhou, Fei Teng, Xijie Sun: School of Civil Engineering, Qingdao University of Technology, Qingdao 266520, China
Jigang Zhang: School of Civil Engineering, Qingdao University of Technology, Qingdao 266520, China; Collaborative Innovation Center of Engineering Construction and Safety in Shandong Blue Economic Zone, Qingdao 266033, China
Changquan Liu: The Third Construction Co.,Ltd, China Construction Eighth Engineering Division, Nanjing 210046, China

of weak interfaces, cracks and breaks, stain residues, low strength concrete, *etc.*, exist in the old structure substrate, for which it is difficult to achieve structural interface repair and rapid strengthening effect with ordinary cement repair mortar. Many scholars studied the repair performance of Portland cement-based repair mortars on the substrate concrete. They found that its bond strength (f_b) on the substrate was not strong, and a non-negligible gap existed when the concrete dried and shrunk at different times, which jeopardized the wholeness between common repair mortars and old substrates [16,17]. Therefore, there is an urgent need to develop a special repair mortar with multi-functional performance such as fast-setting, high strength, low shrinkage, well-compatibility, and superior durability.

It is well known that viscous polymer latex can significantly improve the interfacial bond performance as frequently reported [18–20]. Compared to UHPC or ECC repair materials, the polymer-modified repair materials generally possess superior surface hydrophobic behavior, higher ductility, superior resistance to chloride ion permeability or corrosion, and lower shrinkage, whereas with relatively lower mechanical strength [21–24]. So, polymer-modified repair material is suitable to serve as high-performance cement-based repair materials [25,26]. In the 1980s, Ohama [27] and Konietzko [28] proposed the polymer netlike formation model and the dual web model in cement mortar, respectively. Ohama argued that the polymer would wrap a film around the hardened cement paste, while Grosskurth and Konietzko argued that the polymer and cement paste would interpenetrate and form a network structure. Today there are two main views on polymer-modified cement mortars (PCMs). One is based on the physical behavior of the polymer latex during the hydration of the cement [29,30]. During the hydration process, the polymer creates a network structure on the surfaces of the hydration products and cement particles or fills in the cracks of the cementitious material to improve its pore structure. The other view is that there is a physical interaction and chemical reaction between the polymer latex and the cement hydration, and the chemical reaction is a coordination reaction between Ca^{2+} within the cementitious material and the polymer directly to improve the final performance through chemical bonding [31–37]. Kim [20] compared the bond strength of different materials modified repair mortars. The 28-day bond strength of styrene-butadiene rubber (SBR) modified repair mortar was 29% higher than the control group, which was the best result among all the materials. Yang *et al.* [22] evaluated the chloride permeability and microstructure of Portland cement mortar modified by SBR latex. The study showed that SBR can improve the resistance of cement mortars to chloride ion permeability and can bind hydration products. Jiang *et al.* [23] reported that the mortar mixed with polyacrylate latex (PA) and silica fume (SF) had high bond strength and excellent durability performance compared with the control mortar without PA and SF. It is worth noting that most studies have shown that the mechanical properties of PCMs dosed with some polymer latex in general reduced, especially dramatic decreases in compressive strength (f_c) [38–41]. Tian *et al.* [42] modified cementitious materials by using four organic polymers, namely silicone propylene latex, benzene propylene latex, waterborne epoxy latex, and acrylic latex, and revealed that most types of latex adversely affected the compressive properties of the cementitious materials. The f_c and flexural strength (f_t) of the cementitious materials with 5 wt% dosage of polyacrylic latex decreased by about 28.0–31 MPa and 9.1–6 MPa, respectively. Pei *et al.* [43] tested the mechanical properties of PA-modified mortars with different monomer ratios and found that the f_c of the modified mortar decreased by more than 50% when dosed with methyl methacrylate. Tian *et al.* [44] found that excessive PA addition significantly reduced the mechanical properties of the cement mortar, and the 28 days f_c of mortar specimens mixed with 10 wt% PA was only about 36 MPa. Ma and Li [45] found that the f_c of the mortar dosed with 10% PA decreased by 11.7% compared to the control mortar. Obviously, the f_c of PCM is still eager to substantial enhancement to achieve superior repairing property.

The dense microstructure of cement-based composites is the foundation for achieving high strength, toughness, and durability [46–49]. Therefore, the study of pursuing novel materials to regulate hydration products of cement-based composite has attracted considerable attentions. The employment of carbon nanotubes, graphene oxide (GO), and other materials can effectively toughen the cementitious materials [50–55]. Especially, GO possessing many oxygen-containing functional groups, high surface area, and amphiphilic hybrid sp^2 structure, can exert its active template and nucleation effect at very low dosage [56–59], and it can assume to have the role of template in the hydration products of the cementitious materials, accelerate the hydration rate, reshape the microstructure, and control the distribution of hydration products and form a regular and orderly microstructure [60–64]. Some scholars have found that suitable GO dose can significantly improve the tensile strength [65], f_c and f_t [66] of the cementitious materials, improve the microstructure [67] and durability [68], and reduce the expansion rate [52]. Meanwhile, the functional groups such as hydroxyl, carbonyl, and carboxyl groups of GO itself make it easy to react

with organic polymers, and the reacted GO can also be effectively dispersed in cement matrix to embody its excellent properties in the corresponding composite [69,70].

Here combined with the merits of two kinds of materials, GO/acrylate polymer-modified repair mortar (GOPARMs) by hybridization of GO and PA was first prepared. The f_t, f_c, flexural-compressive strength ratio (f_t/f_c), bond strength, resistance to chloride ion permeability, and microstructure of GOPARMs were also systematically investigated, to evaluate the practicability of GOPARMs as a novel repair material with excellent toughness, adhesion, and resistance to chloride ion permeability.

2 Materials and testing methods

2.1 Materials and mix ratio design

The chemical composition of cement (C), 42.5 grade high-belite sulfur-aluminate cement (HBSAC), produced by Tangshan Polar Bear Cement Plant Co., is shown in Table 1. Sand (S), ordinary river sand, locally available, with fineness modulus of 2.64, medium sand, mud content of less than 1.0% after rinsing treatment, in accordance with the requirements of DL/T 5126-2001 [71] was used. Superplasticizer (Sup), polycarboxylic superplasticizer with 30% water reduction rate, produced by Shandong Academy of Construction Sciences was procured. Polyacrylate latex (PA), obtained from the polymerization of acrylic monomer, was purchased from Beijing Mengtai Weiye Building Materials Co., Ltd, its main characteristics are shown in Table 2. Polyether modified silicone defoamer, B-364 type, was purchased from Guangdong China-union Fine Chemical Co. GO suspension with 10 mg/mL concentration, with 49–56% carbon and 41–50% oxygen content, was purchased from Nanjing Xianfeng Nanomaterials Technology Company. Distilled water (W), homemade was available.

The PA latex and GO dosages were calculated according to the solid content of PA and GO, respectively. The mix ratio was referred to the previous experimental results of Luo *et al.* [72] and fixed at (C + PA):S:W = 1:1.7:0.4 after allowing for the water content in the PA and GO. Table 3 shows the experimental mix ratios and specimen grouping of GOPARMs.

2.2 Test apparatus and instruments

The main apparatus and instruments included: cement mortar mixer with a blade, ISO-679 type, Wuxi Jianding Construction Instrument Factory; TIP Ultrasonic pulverizer, FS-200T type, Shanghai ShengXi Ultrasonic Instrument Co., Ltd; electro-hydraulic universal machine, DYE-300 type, Wuxi Emino Testing Machine Co., Ltd; field emission scanning electron microscope, ISM-7610F type, Japan Electronics Inc.; magnetic stirrer, X85-2 type, Shanghai Meiyingpu Instrument Manufacturing Co., Ltd; electric thermostatic water bath, HHD-2 type, Shanghai Bilang Instrument Manufacturing Co., Ltd; vacuum drying oven, DHG-9030A type, Shanghai Jinghong Experimental Equipment Co., Ltd.

2.3 Preparation and experimental methods

2.3.1 Preparation of GO/PA suspension

The GO dispersion, Sup, and remaining water (total water required for the design ratio minus the water contained in PA and GO) were mixed in a beaker and sonicated for

Table 1: Main chemical composition of HBSAC

Cement type	CaO	SiO_2	Al_2O_3	SO_3	Fe_2O_3	MgO	R_2O	Loss
HBSAC	41.97	18.33	16.63	14.97	1.00	5.34	0.78	0.15

Table 2: Main physicochemical properties of polyacrylate latex

Appearance	Solid content (wt%)	Main monomer	pH	Minimum film-forming temperature (°C)	Vitrification temperature (°C)	Viscosity (MPa s)
Milk-white liquid	55 ± 1	Acrylic acid	7–9	20	105	50

Table 3: Experimental mix ratio design of GOPARMs (unit: kg/m^3)

Item no.#	C	S	PA	GO	W	Sup	Defoamer
P0G0	625	1,063	0	0	250	1.3	0
P5G0			31.3	0	262.5	1.3	0.2
P5G1			31.3	0.065	262.5	1.3	0.2
P5G3			31.3	0.196	262.5	1.3	0.2
P5G5			31.3	0.328	262.5	1.3	0.2
P10G0			62.5	0	275	1.4	0.4
P10G1			62.5	0.068	275	1.4	0.4
P10G3			62.5	0.206	275	1.4	0.4
P10G5			62.5	0.343	275	1.4	0.4
P20G0			125	0	300	1.5	0.8
P20G1			125	0.075	300	1.5	0.8
P20G3			125	0.225	300	1.5	0.8
P20G5			125	0.375	300	1.5	0.8

#Noting, P20G1 means GOPARMs with PA and GO dosage being 20 and 0.01%, respectively, the others are named by analogy.

20 min (sonication power 100 W and frequency 40 kHz); PA was added to the dispersed GO solution and magnetically stirred for 10 min, and the GO/PA suspension was accordingly prepared as reserved.

2.3.2 Preparation of substrate specimens for bond bending test

The bending bond strength (f_b) test was referred to JC/T 2381-2016 [73]. It is worth to note that in order to keep the moisture content and the roughness of bonding interface of the substrate as consistent as possible for different experimental groups of the substrates, we improved to the preparation process of the substrates. The specimen with the size of 40 × 40 × 160 mm was sawed into two splits of 40 × 40 × 80 ± 2 mm blocks using a cutting machine, and the cut surfaces of the test block were lightly polished using an angle grinder to make each cut surface to have the same interface roughness. The polished test blocks were oven-dried at 105 ± 2°C until the weight was unchanged, and then they were immersed in water to saturate, and their saturation rates were calculated. The substrate test blocks were oven-dried at 105 ± 2 °C until its water content was between 55 and 65%. The test blocks were film sealed and left to stand for 2 days.

2.3.3 Preparation of GOPARMs specimens

GOPARMs was prepared according to the pre-designed ratio with reference to the preparation method specified in GB/T17671-1999 [74]. The cement, water, and sand were first mixed at 40 rpm for 2 min at low speed; GO/PA suspension was subsequently mixed into the above mixture for 2 min at low speed, then stirred rapidly at 80 rpm for 30 s, and the defoamer was dipped to eliminate the air bubble; after that, the well-mixed slurry was poured into the molds of varied sizes (40 mm × 40 mm × 160 mm, φ100 mm × 50 mm), vibrated about 60 times on a mortar jump table to compact and facilitate the possible air bubble escaping from the slurry. The mortar surface was smoothed and film covered, and the GOPARMs specimens were removed after 5 h setting and standard curing

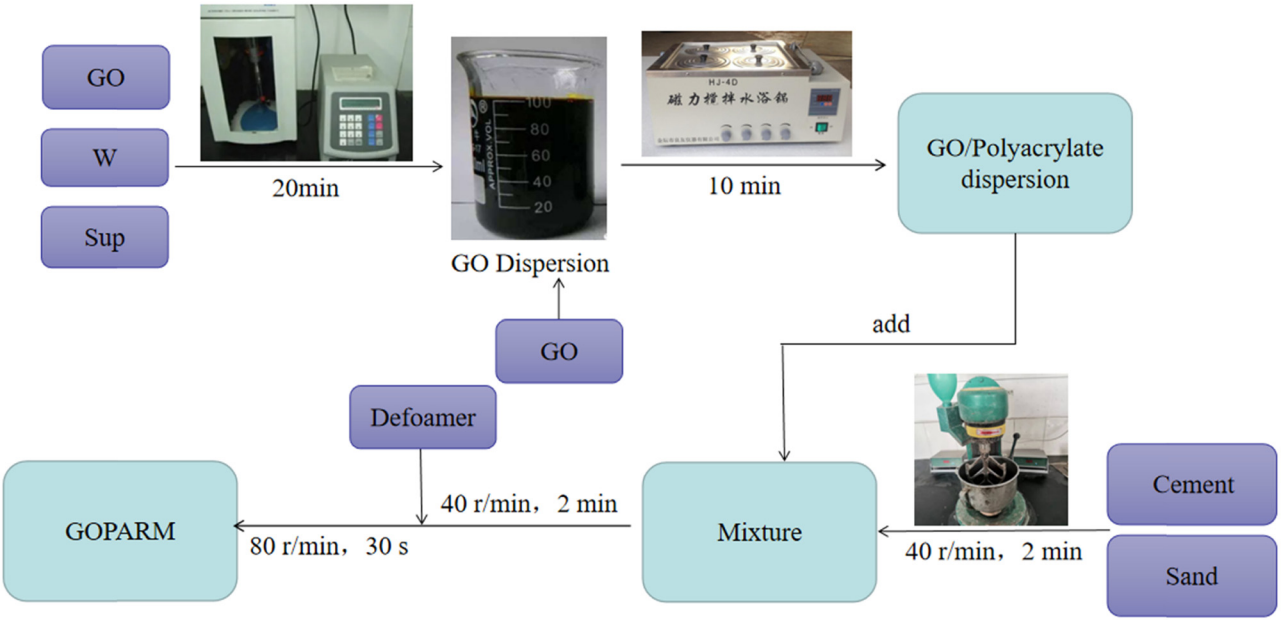

Figure 1: Preparation process of GOPARMs.

Figure 2: Photos of GOPARMs specimens: (a) compressive and flexural strength test (red arrow-prism); (b) resistance to chloride ion permeability test (blue arrow-cylinder); (c) bending bond test (green rectangular-new/old interface).

till 7 days of age. The preparation process of GOPARMs is shown in detail in Figure 1.

2.3.4 Characterization of cured GOPARMs specimens

Compressive and flexural strength tests for the specimens with size of 40 mm × 40 mm × 160 mm was referred to GB/T17671-1999 [74], as shown in Figure 2(a), and the average experimental data of three specimens in each group represent the final result. The resistance to chloride ion permeability test was referred to GB/T50082-2009 [75], as shown in Figure 2(b), and the data are processed in the same way as the previous one. The bending bond strength (f_b) test was referred to JC/T 2381-2016 [73], the f_b was expressed by the interfacial bending strength between GOPARM specimens and old substrates, and tested by testing the f_t of 40 mm × 40 mm × 160 mm specimens bonded by GOPARMs to the substrate specimens. As shown in Figure 2(c), there are six specimens in each group, and the measured data are averaged by possibly removing the maximum and the minimum value with 15% float above or below to the average, and taking the average of the remaining, and the calculation results are accurate to 0.01 MPa.

Finally, some tiny cubes from the fracture section of GOPARMs in No. P0G0 and P5G3 were observed with field-emitting scanning electron microscopy (FESEM) to analyze the effect of PA and GO on the microstructure of the corresponding mortar.

3 Results and discussion

3.1 Mechanical strength

The effects of PA and GO dosage on the mechanical properties (f_cs and f_ts) of GOPARMs are shown in Figure 3.

From Figure 3(a), under the condition of the same GO dosage, the higher the PA dosage is, the lower is

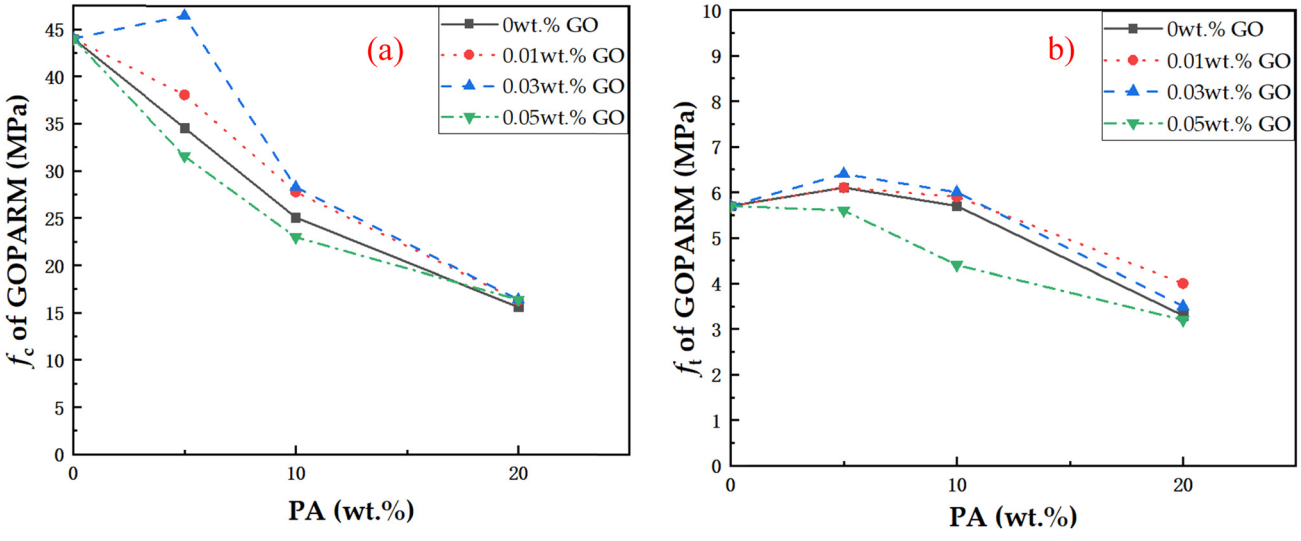

Figure 3: Variation curves of 7 days f_cs and f_ts of GOPARMs with different PA and GO dosages: (a) f_c; (b) f_t.

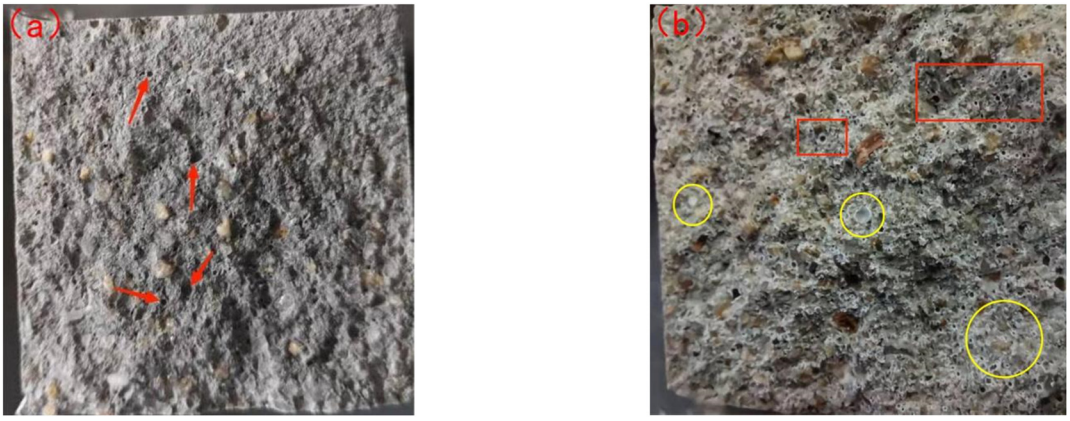

Figure 4: Classic section morphology of GOPARMs: (a) P0G0 group (red arrows–pores); (b) P5G3 group (yellow circles: polymer films and; red rectangles: air bubbles).

the f_c of GOPARMs, when the PA dosage reaches 20 wt%, the f_c of GOPARMs is only about 16 MPa. While under the condition of the same PA dosage, the f_c of GOPARMs increases along with GO dosage. When GO dosing is 0.03 wt% and PA dosing is 5%, the corresponding f_c reaches the maximum value of 46.5 MPa, which is 4.5% higher than that of ordinary mortar without GO or PA dosing (44.5 MPa). And it's noting, the f_c of GOPARMs has somewhat decrease when GO dosage continues to increase.

It can be seen from Figure 3(b) that under the same condition of GO dosage, the f_t of GOPARMs altered with PA dosage is different from that of f_c. In the case of low PA dosage (5 wt%), the f_t of GOPARMs increases, and its f_t reaches the maximum 6.7 MPa when GO dosage is 0.03 wt%, which is almost 20% improvement with respect to the plain mortar (5.6 MPa) without any PA and GO; as the PA dosage continues to increase, the f_t enhancement gradually decreases. And under the same condition of PA dosage, the effect of GO on the f_t of GOPARMs has the same trend as its effect on its f_c. Under the condition of low dosage of PA (lower than 0.03 wt%), the higher the GO dosage is, the higher is the f_t of GOPARMs, whereas when the GO dosage climbs up to 0.05 wt%, the corresponding f_t decreases significantly.

Obviously, at the optimal dosages of 5 wt% PA and 0.03 wt% GO, the corresponding f_c and f_t are 46.5 and 6.4 MPa, respectively.

As known, PA dosage has a negative effect on the f_c of GOPARMs. Actually, with the hydration reaction of cement, PA will form polymer films staggered inside the mortar or wrap the hydration products. As shown in Figure 4(a) and the yellow circles in Figure 4(b), there exists obvious milky white films in the specimens with 5 wt% PA dosage, but not in the control specimen without PA dosage. Because the elastic modulus of the polymer film is much lower than that of the main product C–S–H gel, after the cement mortar is hardened, it leads to the reduction in the elastic modulus, and the f_c of GOPARMs. In addition, the loading of viscous polymer will inevitably introduce air bubbles, as shown by the red rectangles in Figure 4(b). Although appropriate amount of defoamer has been added, still the air-entraining effect of the polymer cannot be avoided, and the introduction of larger pore size bubbles will increase the porosity of the mortar, so the f_c of GOPARMs will have an unignorable drop with high polymer dosage.

It is worth noting that there exists an obvious increase (7%) in f_t of GOPARMs at low PA dosage (0 wt% GO dosage). This is because as the hydration reaction of cement proceeds, PA can form a film inside the mortar to fill the small gaps between or wrap the hydration products, which are attached to the surface of the cementitious gel and improves the bulk flexural strength (f_t) and toughness (f_t/f_c) of the final mortar. When the filling and wrapping effect of the polymer reaches saturation, the f_t of cement mortar reaches the highest. However, if the polymer dosage continues to increase, the hydration products per unit area decreases, resulting in a decrease in the continuity between hydration products per unit area, the polymer will overwhelm the cement particles, thus affecting the hydration degree [45], and the corresponding macroscopic f_c and f_t of the cement mortar decrease. In addition, the air-entraining effect of polymer will also have a negative impact on the f_c and f_t of the cement mortar, as shown by Figure 4(a) and (b). Accordingly, the microstructure in group No. P5G3 specimen has much more air bubbles than that in No. P0G0 group.

Obviously, the increase in f_c and f_t at low GO dosage is owing to the nucleation effect and reshaped microstructure of GO on cement hydration products. It can render AFt, AFm, AH, CH, and C–S–H gel to form regular

and orderly arrangements through the templating effect of GO itself, forming flower-shaped or multifaceted shape crystals or gels [34,62,63]. These crystals or gels mostly grow in the pores or loose positions in the mortar structure and are mutually connected with each other, with the tendency to form a network, which in turn increases the f_c and f_t of the mortar. With the continuous increase in GO dosage, the dispersion effect of GO is insufficient and agglomeration phenomenon may occur, which will lead to the accumulation and irregular arrangement of hydration products, and the bridging capacity between hydration decreases, its f_c and f_t accordingly falls down [64,69].

3.2 Fracture toughness

The fracture toughness of GOPARMs can be characterized by its ratio of f_t/f_c, with higher f_t/f_c indicating superior fracture toughness of the composite [76].

Figure 5 shows the changes in the f_t/f_c of GOPARMs with different dosage of PA and GO. It can be seen that the f_t/f_c of the composite gradually increases with the increase in PA dosage, and the variation in f_t/f_c is great in the range of 0–10 wt% dosage (f_t/f_c increased by 74.6, 63.1, 63.1, and 46.9% at 0, 0.01, 0.03, and 0.05 wt% GO dosage, respectively), while it is relatively low in the range of 10–20 wt% dosage (f_t/f_c increased by - 6.6, 15.6, 0.5, and 2.1% at 0, 0.01, 0.03, and 0.05 wt% GO dosage, respectively). This indicates that the fracture toughness of GOPARMs can be effectively improved with the appropriate dosage of PA. Actually, PA itself has very good deformability, it can well fill the small pores inside the GOPARMs, suitable PA dosage renders GOPARMs to have superior fracture toughness [43].

Figure 5 also shows that there is no significant variation in the f_t/f_c of GOPARMs with GO dosage under the same PA dosage condition. It shows that the GO dosage has no significant effect on the f_t/f_c of GOPARMs. In terms of f_t/f_c, the optimal dosage of PA and GO are 20 and 0.01 wt%, respectively, the corresponding f_t/f_c is 0.245. It should be noted that at this dosage level, the corresponding f_c of GOPARMs decreases significantly owing to low elastic modulus of PA at high dosage.

3.3 Interfacial bond strength

3.3.1 Effect of PA dosage on the f_b of GOPARMs

As shown in Figure 6, the f_b of GOPARMs with the substrate is significantly enhanced by low PA dosage, and the most obvious improvement effect is achieved by 5 wt % PA dosage. Without any GO dosage, the f_b of GOPARMs increases by about 39% with respect to the baseline; whereas with the addition of 0.03 wt% GO, the f_b reaches the maximum value (6.73 MPa), which is about 103% enhancement compared with the baseline group. It is worth to note that with higher PA dosage, the increment amplitude of f_b of the GOPARMs also decreases. When the PA dosage is 10 wt%, the f_b of the specimens without GO dosage increases by about 36% compared with the baseline; when the GO dosage is 0.03 wt%, it accordingly increases by about 45% compared with the baseline. While the f_b of the specimens is even lower than that of the baseline when the PA dosage reaches 20 wt%.

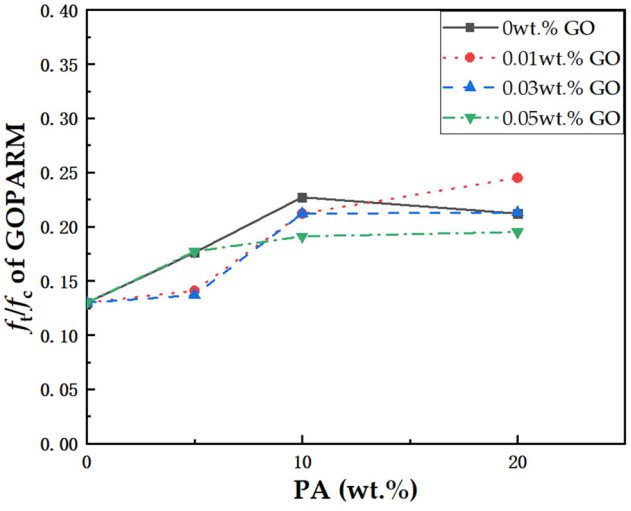

Figure 5: Variation curve of 7 days f_t/f_c of GOPARMs with different PA and GO dosages.

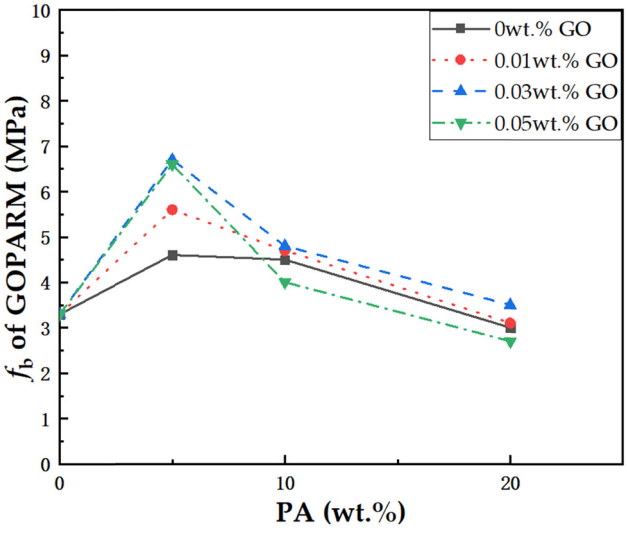

Figure 6: 7 days f_b change in GOPARMs along with different PA and GO dosages.

Figure 7: RCM test procedure of GOPARMs: (a) rubber sleeve installation; (b) power penetration; (c) section color change after spraying silver nitrate.

The f_b of mortar with low PA dosage increases because the polymer in the mortar can penetrate into the pores of the mortar, rendering the contact surface of the old and new test blocks more tightly connected, so the f_b of the mortar will be elevated. When PA dosage keeps increasing, the content of the cementitious material in the mortar decreases and the polymer content increases, the bonding performance of the cement mortar decreases when the f_b of the cementitious material decreases to a greater extent than the f_b provided by the polymer.

3.3.2 Effect of GO on the f_b of GOPARMs

From Figure 6, the f_b of GOPARMs and the substrate will be enhanced with a small amount of GO, and the enhancement effect on the f_b of GOPARMs is related to PA dosage. The best strengthening effect of GO on the f_b of the specimen can be achieved when the PA dosage is 5 wt%, and the f_b gradually increases up to 6.73 MPa when the GO dosage is between 0 and 0.03 wt%. While GO dosage continues to increase, the corresponding f_b steadily decreases. Under the condition of 10 wt% PA dosage, the f_b gradually increases up to 4.82 MPa when GO dosage is between 0 and 0.03 wt%, and when the GO dosage continues to increase, the f_b starts to decrease, and sharply drops down to 4.00 MPa. Under the condition of 20 wt% PA dosage, the GO dosage has no obvious effect on the improvement of the bonding performance, and even causes a significant decrease in the f_b.

The mechanism of GO enhancing the f_b of GOPARMs is similar to that of enhancing the f_c of GOPARMs, which can induce the generation of flower-shaped and polyhedral crystals at the pores and cracks in the cementitious composites, thereby reduce the pores and cracks, and significantly improve the strength, toughness, and interface adhesion of the mortar.

In terms of f_b, 5 wt% PA and 0.03 wt% GO are the optimal dosage, for the f_b of GOPARMs to reach up to 6.73 MPa.

3.4 Chlorine ion permeation resistance performance of GOPARMs

Figure 7 shows the rapid chloride ion migration coefficient method (RCM) test operation and the color rendering diagram of chloride ion permeation of specimens. Seven groups of specimens were selected for this test, namely No. P0G0, P5G0, P5G1, P5G3, P5G5, P10G0, and P20G0, and the mix ratios of each group are shown in Table 3. The effect of GO and PA dosages on the resistance to chloride ion permeability of mortar was investigated by analyzing the chloride ion migration coefficients (λ_c) of No. P5G0, P5G1, P5G3, P5G5, P0G0, P10G0, and P20G0, respectively.

The λ_c is calculated according to equation (1):

$$D_{RCM} = \frac{0.0239 \times (273 + T)L}{(U - 2)t} \times \left(X_d - 0.0238\sqrt{\frac{(273 + T)LX_d}{U - 2}} \right), \quad (1)$$

where, D_{RCM} – non-stationary λ_c of concrete, accurate to 0.1×10^{-12} m^2/s; U – absolute value of the voltage used (V); T – average of the initial and ending temperatures of the anode solution (°C); L – specimen thickness (mm), accurate to 0.1 mm; X_d – average value of chloride ion penetration depth (mm), accurate to 0.1 mm; t – test duration (h).

3.4.1 Effect of PA dosage on the resistance to chloride ion permeability of GOPARMs

As seen from Figure 8, with the increase in PA dosage, the λ_c first gradually decreases, and when the PA dosage

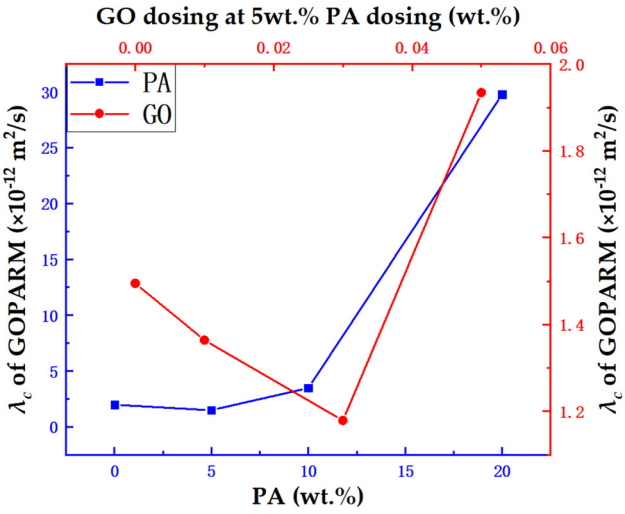

Figure 8: Effect of PA and GO dosage on the λ_c of GOPARMs.

increases to 5 wt% (GO dosage 0), the λ_c is the smallest, only 1.495 × 10^{-12} m^2/s, which is 24.3% less than that of the specimens without PA dosage (P0G0). Continuing to increase the PA dosage, the λ_c of GOPARMs gradually increases, and when the PA dosage reaches 20 wt% (GO dosage 0.03 wt%), the λ_c reaches 29.763 × 10^{-12} m^2/s, which is much larger than that of the blank group. Therefore, an adequate amount of PA can improve the resistance to chloride ion permeability of mortar to a certain extent, but too large PA dosage will have a negative effect on the impermeability of the mortar.

The reason why fewer PA can increase the resistance to chloride ion permeability of mortar is that the polymer can penetrate into the pores of the mortar, and cement hydration absorbs the water from outside and the water in PA. The organic polymer film can be formed after the PA dries, and this film has a good filling effect on the small pores and improves the material resistance to chloride ion penetration. It is worth noting that the addition of too much PA will make the mortar very viscous, and many larger air bubbles will be introduced during the preparation of mortar specimens, which leads to a reduction in the compactness and resistance to chloride ion permeability.

3.4.2 Effect of GO dosage on the resistance to chloride ion permeability of GOPARMs

From Figure 8, we can clearly observe that with the increase in GO dosage, the λ_c decreased first, and the smallest λ_c of 1.179 × 10^{-12} m^2/s was obtained when the GO dosage was 0.03 wt% (PA dosage 5 wt%), which was about 13.6% lower than that of the P5G0 group without GO dosage. However, when the GO dosage was increased to 0.05 wt%, the λ_c increased again to 1.934 × 10^{-12} m^2/s, which was 41.8% higher than that of P5G0. The above experimental phenomenon indicates that the addition of a small amount of GO can reduce the λ_c of the specimens, *i.e.*, the resistance to chloride ion permeability is improved, but the excessive amount of GO will adversely affect the resistance to chloride ion permeability of the specimens.

The effect of change in GO on the microstructure of mortar can explain the above situation well. Low amount of GO has good active template and nucleation effect, which can effectively improve the arrangement structure of hydration products, reduce the pore structure inside GOPARMs, and improve the impermeability of the mortar. Excessive amount of GO is not easy to disperse in the cementitious materials, and agglomerated GO cannot play its excellent performance, but will lead to the agglomeration and accumulation of hydration products, reduce the connection between hydration crystals, and the internal compactness of GOPARMs to be reduced, which is not conducive to its impermeability performance.

In terms of the resistance to chloride ion permeability, 5 wt% PA and 0.03 wt% GO are the optimal dosage, respectively, and the corresponding λ_c of GOPARMs is 1.179 × 10^{-12} m^2/s.

3.5 Micromorphological analysis of GOPARMs

In order to observe the microscopic morphology of GOPARMs and further verify the microscopic mechanism of the changes in its mechanical properties, bonding properties, and resistance to chloride ion penetration, in this study, the cross-sections were observed by field-emitting scanning electron microscopy.

3.5.1 Micromechanical analysis of PA to improve the performance of GOPARMs

Figure 9 shows the microscopic morphology of hydration products of GOPARMs with different PA admixtures. The blank group in Figure 9(a) shows typical cement hydration products, including needle-rod AFt, amorphous AFm, CH, AH, and bulk C–S–H gels with a relatively loose structure and more voids and cracks. In Figure 9(b), with PA dosage of 5 wt%, PA has obviously played a role in filling the pores and connecting the hydration products, the gel

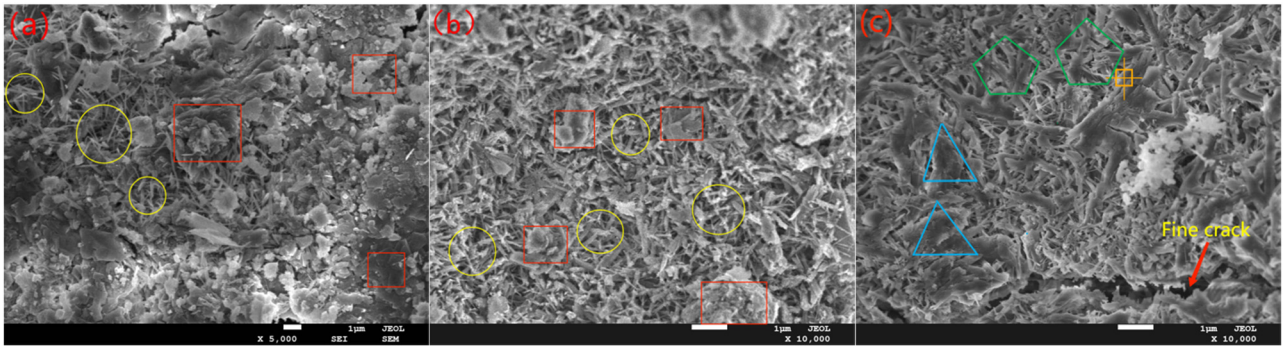

Figure 9: Morphology of hydration products of GOPARMs with different PA dosage (yellow circles: AFt; red rectangles: other amorphous hydration products; green pentagon: AFt wrapped in PA; blue triangles: agglomerates composed of hydration products and PA): (a) without PA dosage; (b) PA dosage 5 wt%; (c) PA dosage 10 wt%.

Table 4: EDS analysis of PA modified mortars from Figure 9(c) (wt%)

Chemical element	C	O	Al	Si	S	Ca
Atom content (wt%)	9.3	71.5	5.1	1.9	4.6	7.6

structure is obviously denser compared to the blank group, and the polymer starts to form a small amount of encapsulation on the hydration products. In Figure 9(c), the presence of continuous rod-like gels can be clearly observed with PA dosage of 10 wt%, and these gels are mixed gels of polymer and hydration products, *i.e.*, the polymer has obvious encapsulation connection to the needle and rod-like hydration products. However, some of the gels intertwined with the cement hydration products appeared to be agglomerated into clumps, which produced fine cracks compared to GOPARMs with 5 wt% PA dosage.

The results of the different elemental contents detected in the orange marked points of PA-modified mortars in Figure 9(c) are given in Table 4. It can be found that the C/O is about 0.13, which is much higher than the C/O of ordinary cementitious materials [34]. Moreover, Ca, Si, S, and Al in the mortars, which are the key elements that constitute the hydration products of SAC, can also be detected by EDS. The junction and the EDS and SEM test results can prove that the hydration products of the cementitious materials and PA mixed with each other. And PA can fill the voids between the hydration products or encapsulate the hydration products.

After microscopic tests, it is difficult to observe a very obvious polymer film formation regardless of the PA dosage, and it is speculated that the improving mechanism of the PA on the performance is not the one proposed by most scholars to enhance the macroscopic performance of mortar by forming a good integral polymer film between hydration products [77–79]. Tian *et al.* [34] demonstrated that PA can complexation react with Ca^{2+} within the cementitious materials to generate calcium carboxylate functional groups, which can enhance the properties of the cementitious materials through chemical bonding. In summary, a small amount of PA can not only improve the compactness of mortar material by filling the internal pores of GOPARMs

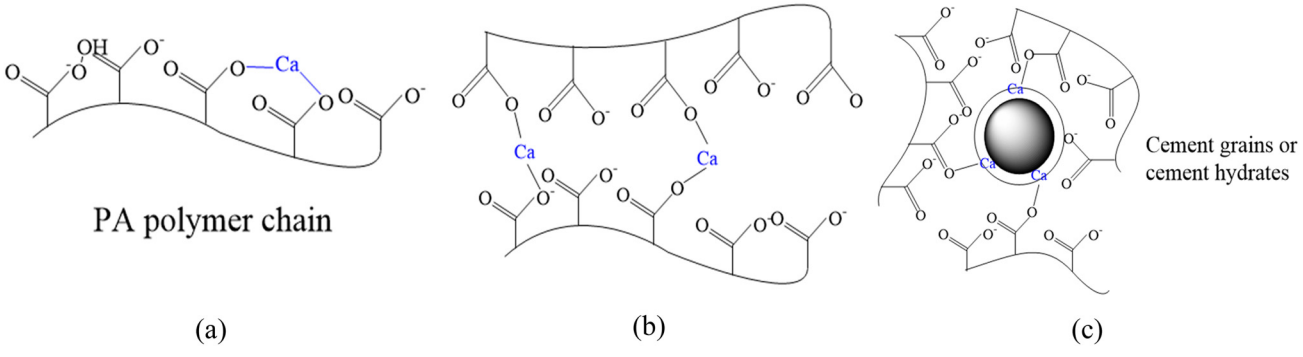

Figure 10: Reactions between Ca^{2+} and polyacrylate (PA) polymer chain: (a) self-link of polymer chain; (b) cross-link of PA polymer chains; (c) cross-link between PA polymer chain and cement hydrates.

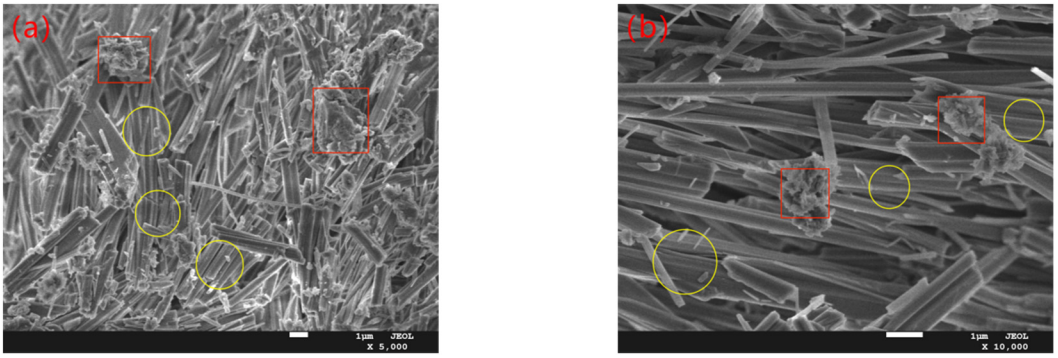

Figure 11: Morphology of hydration products of GOPARMs doped with 0.03 wt% GO (very dense and orderly distribution of hydration products): (a) ×5k; (b) ×10k (yellow circles: AFt and red rectangles: other amorphous hydration products).

but also enhance the material properties by forming ligand bonds through chemical reactions, the specific complexation reactions are shown in Figure 10. However, the large amount of PA will lead to the increase in large internal pores due to the air-entraining effect of PA, which will reduce the degree of material compactness and adversely affect the performance of GOPARMs.

3.5.2 Micromechanical analysis of GO to improve the performance of GOPARMs

Some scholars have found that GO can be modified by Sup or PA through non-covalent or covalent bonding modifications during physical mixing [69,80,81]. It can effectively improve the dispersion of GO, which is the basis for GO to exert its excellent performance [82].

Figure 11 shows the morphology of hydration products of GOPARMs doped with 0.03 wt% GO. It can be clearly seen that the internal hydration products of mortar are denser and more orderly after GO dosage. This will lead to a significant increase in the denseness of the cement mortar material, which is beneficial to the improvement of the macroscopic properties of the material. The dense and orderly distribution of hydration products is due to the small amount of GO in GOPARMs which exerts active template and nucleation effect. The high specific surface area of GO provides a good nucleation structure for the orderly growth of hydration products, and GO itself can also play a good filling and linking effect between hydration products and cement particles, optimizing the three-dimensional network structure inside GOPARMs. Therefore, GO can play a good toughening and densification effect on GOPARMs, which can effectively improve the mechanical properties and impermeability of the material [83–86].

It is concluded that all the properties of GOPARMs meet the specification requirements, and its f_b and λ_c are significantly superior to those of the ordinary repair mortar, which is suitable as a cost-effective repair and reinforcement material application in concrete structure.

4 Conclusion

In this article, GO dispersion and PA were physically blended and the GO/PA mixture was synergistically modified cement mortar, and the mortar was characterized with mechanical and durability behavior (f_c, f_t, f_t/f_c, f_b, and λ_c). Some results are concluded:

1) With the increase in PA dosage, the f_c of mortar steadily decreases, and the f_t/f_c steadily increases, but the f_t, f_b, and λ_c of the mortar first increases and then decreases.
2) With the increase in GO dosage, the f_c, f_t, and f_b of mortar are all up first and then down, yet the trend of f_t/f_c is not obvious, the optimal GO dosage is at 0.03 wt%.
3) The doped GO can play an active template and nucleation effect among the hydration products of GOPARMs, resulting in improved texture and microstructure; while the doped PA can encapsulate the hydration products to a certain extent, playing the role of filling the internal pores and connections, and forming coordination bonds between the hydration products, thereby improving the mechanical toughness, bonding, and resistance to chloride ion permeability of GOPARMs.
4) After comprehensive consideration, the f_c, f_t, f_t/f_c, f_b, and λ_c of GOPARMs with the dosage of 5 wt% PA and 0.03 wt% GO reach 46.5 MPa, 6.4 MPa, 0.14, 6.73 MPa, and 1.179×10^{-12} m^2/s, respectively, which are enhanced by 5.7, 12.3, 7, and 103%, and the corresponding λ_c is

reduced by 40.4%. Obviously, a cost-effective and competitive repair mortar with superior bonding and resistance to chloride ion permeability can be predicted.

Acknowledgments: The authors are obliged to thank for the reinforcement mechanism discussion with Prof. Qiuyi Li (Qingdao Agriculture University) and Prof. Jing Zhong (Harbin Institute of Technology (Shenzhen)).

Funding information: This study was financially supported by NSFC-Shandong Province Joint Key Project (Grant No. U2106222), National Natural Science Foundation of China (No. 51878364), Key Technology Research and Development Program of Shandong Province (Public welfare type) (No. 2019GSF110008), and the National "111" project, and Gaofeng discipline project funded by Shandong Province.

Author contributions: Jianlin Luo, Jigang Zhang: conceptualization, supervision, and resources; Yibo Gao, Jianlin Luo, and Xijie Sun: data curation, formal analysis, and methodology; Jianlin Luo, Changquan Liu, and Jigang Zhang: funding acquisition, investigation, and project administration; Yibo Gao and Jianlin Luo: validation, visualization, and writing - original draft; Yibo Gao, Jianlin Luo, Fei Teng, and Xiaoyang Zhou: writing - review and editing. All authors have accepted responsibility for the entire content of this manuscript and approved its submission.

Conflict of interest: The authors state no conflict of interest.

References

[1] Pavlíková M, Zemanová L, Záleská M, Pokorný J, Lojka M, Jankovský O, et al. Ternary blended binder for production of a novel type of lightweight repair mortar. Mater. 2019;12(6):996.
[2] Xia Q, Wen J, Tang X, Zhu Y, Xu Z, Du Z, et al. Optimal preparation and degradation characterization of repair mortar containing waterborne epoxy resin emulsions. Constr Build Mater. 2021;298:123839.
[3] Yang J, Wang R, Zhang Y. Influence of dually mixing with latex powder and polypropylene fiber on toughness and shrinkage performance of overlay repair mortar. Constr Build Mater. 2020;261:120521.
[4] Zanotti C, Borges PHR, Bhutta A, Banthia N. Bond strength between concrete substrate and metakaolin geopolymer repair mortar: effect of curing regime and PVA fiber reinforcement. Cem Concr Compos. 2017;80:307–16.
[5] Jia L, Zhao F, Yao K, Du H. Bond performance of repair mortar made with magnesium phosphate cement and ferroaluminate cement. Constr Build Mater. 2021;279:122398.1–10.
[6] Oh H, Lee I. A Hardening and strength properties of magnesium phosphate mortars for rapid repair materials. J Korea Inst Struct Maintenance Inspection. 2019;23(3):103–10.
[7] Feng S, Xiao H, Geng J. Bond strength between concrete substrate and repair mortar: effect of fibre stiffness and substrate surface roughness. Cem Concr Compos. 2020;114:103746.
[8] He J, Bu X, Bai W, Zheng W, Gao Q, Wang Y. Preparation and properties of self-compacting alkali-activated slag repair mortar. Constr Build Mater. 2020;252:119034.
[9] He Y, Zhang X, Hooton RD, Zhang X. Effects of interface roughness and interface adhesion on new-to-old concrete bonding. Constr Build Mater. 2017;151:582–90.
[10] Okamoto PA, Whiting D. Use of maturity and pulse velocity techniques to predict strength gain of rapid concrete pavement repairs during curing period. Transport Res Rec. 1994;1458:85–90.
[11] Chaunsali P, Mondal P. Physico-chemical interaction between mineral admixtures and OPC-calcium sulfoaluminate (CSA) cements and its influence on early-age expansion. Cem Concr Res. 2016;80:10–20.
[12] Pelletier L, Winnefeld F, Lothenbach B. The ternary system Portland cement-calcium sulphoaluminate clinker-anhydrite: hydration mechanism and mortar properties. Cem Concr Compos. 2010;32(7):497–507.
[13] Li J, Ji YS, Xu ZS. Microstructure evolution of interface between magnesium ammonium phosphate cement and Portland cement under sulphate corrosion environment. Sādhanā Published Ind Acad Sci. 2020;45(3):37–40.
[14] Park JW, Kim KH, Ann KY. Fundamental properties of magnesium phosphate cement mortar for rapid repair of concrete. Adv Mater Sci Eng. 2016;2016:1–7.
[15] Qin J, Qian J, You C, Fan Y, Li Z, Wang H. Bond behavior and interfacial micro-characteristics of magnesium phosphate cement onto old concrete substrate. Constr Build Mater. 2018;167:166–76.
[16] Courard L, Lenaers JF, Michel F, Garbacz A. Saturation level of the superficial zone of concrete and adhesion of repair systems. Constr Build Mater. 2010;25(5):2488–94.
[17] Kim G, Kim JY, Kurtis KE, Jacobs LJ. Drying shrinkage in concrete assessed by nonlinear ultrasound. Cem Concr Res. 2017;92:16–20.
[18] Chung DDL. Use of polymers for cement-based structural materials. J Mater Sci. 2004;39(9):2973–8.
[19] Al-Zahrani MM, Maslehuddin M, Al-Dulaijan SU, Ibrahim M. Mechanical properties and durability characteristics of polymer-modified and cement-based repair materials. Cem Concr Compos. 2003;25(4):527–37.
[20] Kim MO. Influence of polymer types on the mechanical properties of polymer-modified cement mortars. Appl Sci. 2020;10(3):1061.
[21] Lin JS. Preparation and properties of fiber-reinforced polymer cement waterproof slurry [dissertation]. Guangdong: South China University of Technology; 2015 (in Chinese).
[22] Yang Z, Shi X, Creighton AT, Peterson MM. Effect of styrene–butadiene rubber latex on the chloride permeability and microstructure of Portland cement mortar. Constr Build Mater. 2009;23(6):2283–90.
[23] Jiang C, Huang S, Gao P, Chen D. Experimental study on the bond and durability properties of mortar incorporating polyacrylic ester and silica fume. Adv Cem Res. 2018;30(2):56–65.

[24] Xie T, Fang C, Mohamad Ali MS, Visintin P. Characterizations of autogenous and drying shrinkage of ultra-high performance concrete (UHPC): an experimental study. Cem Concr Compos. 2018;91:156–73.
[25] Shi C, Wang P, Ma C, Zou X, Yang L. Effects of SAE and SBR on properties of rapid hardening repair mortar. J Build Eng. 2021;35:102000.
[26] Kong XM, Wu CC, Zhang YR, Li JL. Polymer-modified mortar with a gradient polymer distribution: preparation, permeability, and mechanical behaviour. Constr Build Mater. 2013;38:195–203.
[27] Ohama Y. Handbook of polymer-modified concrete and mortars: properties and process technology. London: William Andrew; 1995.
[28] Grosskurth KP, Konietzko A. Structure and mechanical behaviour of polymer modified cement concrete. Proceeding of 5th International Congress on Polymers in Concrete. Brighton, UK: 1987. p. 171–4.
[29] Mansur AAP, Santos DB, Mansur HS. A microstructural approach to adherence mechanism of poly(vinyl alcohol) modified cement systems to ceramic tiles. Cem Concr Res. 2007;37(2):270–82.
[30] Afridi MUK, Ohama Y, Demura K, Iqbal MZ. Development of polymer films by the coalescence of polymer particles in powdered and aqueous polymer-modified mortars. Cem Concr Res. 2003;33(11):1715–21.
[31] Jenni A, Zurbriggen R, Holzer L, Herwegh M. Changes in microstructures and physical properties of polymer-modified mortars during wet storage. Cem Concr Res. 2006;36(1):79–90.
[32] Ma H, Tian Y, Li Z. Interactions between organic and inorganic phases in PA-and PU/PA-modified-cement-based materials. J Mater Civ Eng. 2011;23(10):1412–21.
[33] Tian Y, Jin X, Jin N, Zhao R, Li Z, Ma H. Research on the microstructure formation of polyacrylate latex modified mortars. Constr Build Mater. 2013;47:1381–94.
[34] Tian Y, Li Z, Ma H, Jin N, Jin NG. An investigation on the microstructure formation of polymer modified mortars in the presence of polyacrylate latex. Proceedings of International RILEM Conference on Advances in Construction Materials Through Science and Engineering; 2011. p. 71–7.
[35] Matsuyama H, Young JF. Synthesis of calcium silicate hydrate/polymer complexes: part I, Anionic and nonionic polymers. J Mater Res. 1999;14(8):3379–88.
[36] Bonapasta AA, Buda F, Colombet P. Interaction between Ca ions and poly (acrylic acid) chains in macro-defect-free cements: a theoretical study. Chem Mater. 2000;13(1):67–70.
[37] Bonapasta AA, Buda F, Pierre C. Cross-linking of poly(vinyl alcohol) chains by Ca ions in macro-defect-free cements. Chem Mater. 2002;14(3):1016–22.
[38] Heng YY, Zhao WJ. Research progress on the properties and mechanism of SAEE modified cement based materials. Bulletin of the Chinese Ceramic Society. 2014;33(06):1431–8 (in Chinese).
[39] Li Y, Zhu JC, Wu YS. Effect of polymer on performance of ultra-high toughness cementitious composites. J Build Mater. 2018;21(1):26–32.
[40] Wang R, Wang PM, Li XG. Physical and mechanical properties of styrene–butadiene rubber emulsion modified cement mortars. Cem Concr Res. 2005;35(5):900–6.
[41] Bahranifard Z, Tabrizi FF, Vosoughi AR. An investigation on the effect of styrene-butyl acrylate copolymer latex to improve the properties of polymer modified concrete. Constr Build Mater. 2019;205:175–85.
[42] Tian YL, Gao PW, Wang R, Wang LM, Zhong JJ, Li JS. Study on the influence of organic polymers on the physical and mechanical properties of cement-based materials, Tokyo University of Science, Tongji University. Proceedings of the 2nd International Conference on Environmental Prevention and Pollution Control Technologies (EPPCT2020). Tokyo University of Science, Tongji University: International Conference on Humanities and Social Science Research; 2020. p. 7.
[43] Pei M, Wu Y, Kim W, Wu Y, Kim W, Hyung W, et al. Effect of the monomer ratio on the properties of poly (methyl methacrylate butyl acrylate) latex-modified mortars. J Appl Polym Sci. 2004;93(5):2403–9.
[44] Tian Y, Li ZJ, Jin XY. Mechanical characterization of polyacrylate emulsion modified mortars. Earth and space 2010: engineering, science, construction, and operations in challenging environments; 2010. p. 3567–78.
[45] Ma H, Li Z. Microstructures and mechanical properties of polymer modified mortars under distinct mechanisms. Constr Build Mater. 2013;47:579–87.
[46] Shi JY, Liu BJ, Qin JL, Jang JY, Wu X, Tan JX. Experimental study of performance of repair mortar: evaluation of *in-situ* tests and correlation analysis. J Build Eng. 2020;31:101325.
[47] Gao S, Li QY, Li N, et al. Research on super dense recycled mortar preparation based on densified parking theory. J Build Struc. 2021;42(S1):466–72.
[48] Yang CJ. Research on properties and repair test of nano-modified polymer cementitious material [dissertation]. Zhejiang: Zhejiang University; 2016 (in Chinese).
[49] Niaki MH, Fereidoon A, Ahangari MG. Experimental study on the mechanical and thermal properties of basalt fiber and nanoclay reinforced polymer concrete. Compos Struc. 2018;191:231–8.
[50] Lu H, Yao Y, Huang WM, Hui D. Noncovalently functionalized carbon fiber by grafted self-assembled graphene oxide and the synergistic effect on polymeric shape memory nanocomposites. Compos Part B. 2014;67:290–5.
[51] Cui HZ, Yang JM, Li JZ. Research progress on carbon nanotubes dispersion techniques and CNTs-reinforced cement-based materials. Mater Rep. 2016;30(2):91–5 (in Chinese).
[52] Luo J, Zhou C, , Li W, Chen S, Habibnejad Korayem A, Duan W. Using graphene oxide to improve physical property and control ASR expansion of cement mortar. Constr Build Mater. 2021;308:125006.
[53] Luo J, Chen S, Li Q, Liu C, Gao S, Zhang J, et al. Influence of graphene oxide on mechanical properties, fracture toughness, and microhardness of recycled concrete. Nanomaterials. 2019;9:325–38.
[54] Zhao Z, Qi T, Zhou W, Hui D, Xiao C, Qi J, et al. A review on the properties, reinforcing effects, and commercialization of nanomaterials for cement-based materials. Nanotechnol Rev. 2020;9:303–22.
[55] Daghash SM, Soliman EM, Kandil UF, Reda Taha MM. Improving impact resistance of polymer concrete using CNTs. Int J Concr Struct Mater. 2016;10(4):539–53.

[56] Zhu Y, Murali S, Cai W, Murali S, Cai W, Li X, et al. Graphene and graphene oxide: synthesis, properties, and applications. Adv Mater. 2010;22(35):3906–24.
[57] Ramezanzadeh M, Ramezanzadeh B, Sari MG, Ramezanzadeh B, Sari MG, Saeb MR. Corrosion resistance of epoxy coating on mild steel through polyamidoamine dendrimer-covalently functionalized graphene oxide nanosheets. J Ind Eng Chem. 2020;82:290–302.
[58] Shen L, Zou L, Ding M, Zou L, Ding M, Zhao T, et al. Investigation of physical properties of epoxy-functionalized graphene nanoplatelets composite coatings on DC-GIL insulators by molecular dynamics simulation. Appl Surf Sci. 2020;505:144197.
[59] Wu X, Field RW, Wu JJ, Field RW, Wu JJ, Zhang K. Polyvinylpyrrolidone modified graphene oxide as a modifier for thin film composite forward osmosis membranes. J Membr Sci. 2017;540:251–60.
[60] Guo SY, Zhang X, Chen JZ, Mou B, Shang HS, Wang P, et al. Mechanical and interface bonding properties of epoxy resin reinforced Portland cement repairing mortar. Constr Build Mater. 2020;264:120715.
[61] Zhao L. Effect of PC modified GO on the reinforcement of cement composites [dissertation]. Jiangsu: Southeast University; 2018 (in Chinese).
[62] Li X, Liu YM, Li WG, Li CY, Sanjayan JG, Duan WH, et al. Effects of graphene oxide agglomerates on workability, hydration, microstructure and compressive strength of cement paste. Constr Build Mater. 2017;145:402–10.
[63] Li W, Li X, Chen SJ, Liu YM, Duan WH, Shah SP. Effects of graphene oxide on early-age hydration and electrical resistivity of Portland cement paste. Constr Build Mater. 2017;136:506–14.
[64] Lu Z, Chen B, Leung CY, Li Z, Sun G. Aggregation size effect of graphene oxide on its reinforcing efficiency to cement based materials. Cem Concr Compos. 2019;100:85–91.
[65] Li X, Lu Z, Chuah S, Li W, Liu Y, Duan WH, et al. Effects of graphene oxide aggregates on hydration degree, sorptivity, and tensile splitting strength of cement paste. Compos Part A. 2017;100:1–8.
[66] Hu M, Guo J, Fan J, li P, Chen D. Dispersion of triethanolamine-functionalized graphene oxide (TEA-GO) in pore solution and its influence on hydration, mechanical behavior of cement composite. Constr Build Mater. 2019;216:128–36.
[67] Wang J, Xu Y, Wu X, Xu Y, Wu X, Zhang P, et al. Advances of graphene and graphene oxide modified cementitious materials. Nanotechnol Rev. 2020;9:465–77.
[68] Wang JK. Study on properties of graphene oxide modified cement-based composites materials [dissertation]. Hebei: Hebei University of Technology; 2018 (in Chinese).
[69] Lv SH, Zhu LL, Jia CM, Li Y, He YY, Zhao HR. Influence of PCs/GO Composites on Microstructure and Mechanical Properties of Cement Based Materials. Mater Rev. 2017;31(06):125–9 + 135.
[70] Wajid AS, Ahmed HST, Das S, Irin F, Jankowski AF, Green MJ. High-performance pristine graphene/epoxy composites with enhanced mechanical and electrical properties. Macromol Mater Eng. 2013;298(3):339–47.
[71] Test code on polymer-modified cement mortar (DL/T 5126-2001). Beijing: China Electric Power Press; 2001 (in Chinese).
[72] Li H, Luo JL, Li QY, Liu C, Chen SC. Bonding repair and shrinkage durability of ductile fiber-reinforced polymer mortar. New Chem Mater. 2019;47(7):266–70 (in Chinese).
[73] Repairing mortar (JC/T 2381-2016). Beijing: China Architecture & Building Press, 2016 (in Chinese).
[74] Method of testing cements-Determination of strength (GB/T 17671-1999). Beijing: Standards Press of China; 1999 (in Chinese).
[75] Standard for test methods of long-term performance and durability of ordinary concrete (GB/T 50082-2009). Beijing: China Architecture & Building Press; 2009 (in Chinese).
[76] Luo J, Li Q, Zhao T, Gao S, Sun S. Bonding and toughness properties of PVA fibre reinforced aqueous epoxy resin cement repair mortar. Constr Build Mater. 2013;49:766–71.
[77] Li B, Tian Y, Zhao RY, Duan A, Li ZJ, Ma HY. Microstructure and modification mechanism of polyacrylate latex modified motars. Journal of Zhejiang University. 2014;48(08):1345–52 + 1361 (in Chinese).
[78] Plank J, Gretz M. Study on the interaction between anionic and cationic latex particles and Portland Cement. Colloids Surf A. 2008;330(2):227–33.
[79] Afridi MUK, Ohama Y, Demura K, Iqbal MZ. Development of polymer films by the coalescence of polymer particles in powdered and aqueous polymer-modified mortars. Cem Concr Res. 2003;33(11):1715–21.
[80] Zhang WB. Preparation and properties of polyacrylate/modified graphene oxide composites [dissertation]. Shanxi: Shanxi University of Science and Technology; 2016 (in Chinese).
[81] Wang D, Zhang X, Zha JW, Zhao J, Dang ZM, Hu GH. Dielectric properties of reduced graphene oxide/polypropylene composites with ultralow percolation threshold. Polym. 2013;54(7):1916–22.
[82] Gao Y, Jing HW, Chen SJ, Du MR, Chen WQ, Duan WH. Influence of ultrasonication on the dispersion and enhancing effect of graphene oxide–carbon nanotube hybrid nanoreinforcement in cementitious composite. Compos Part B. 2019;164:45–53.
[83] Lv S, Ma Y, Qiu C, Sun T, Liu J, Zhou Q. Effect of graphene oxide nanosheets of microstructure and mechanical properties of cement composites. Constr Build Mater. 2013;49:121–7.
[84] Lv SH, Liu JJ, Qiu CC, Ma YJ, Zhou QF. Microstructure and mechanism of reinforced and toughened cement composites by nanographene oxide. J Funct Mater. 2014;45(04):4084–9.
[85] Babak F, Abolfazl H, Alimorad R, Parviz G. Preparation and mechanical properties of graphene oxide: cement nanocomposites. Sci World J. 2014;276233:1–10.
[86] Saafi M, Tang L, Fung J, Rahman M, Liggat J. Enhanced properties of graphene/fly ash geopolymeric composite cement. Cem Concr Res. 2015;67:292–9.